Conversion of model C₆–C₉ alkanes and straight-run gasoline over Pt(0.1%)-Fe(5%)/Al₂O₃ catalysts promoted with various additives

Arai K. Zhumabekova [a] [iD], Lyazzat K. Tastanova [b*] [iD], Raigul O. Orynbassar [c] [iD], Yermek A. Aubakirov [c] [iD], Elvira B. Zhunusova [a]

a: Chemistry, Chemical Technology and Ecology Department, Kazakh University of Technology and Business, Nur-Sultan 010000, Kazakhstan
b: Chemistry and Chemical Technology Department, K. Zhubanov Aktobe Regional University, Aktobe 030000, Kazakhstan
c: Department of Physical Chemistry, Catalysis and Petrochemistry, Al-Farabi Kazakh National University, Almaty 050040, Kazakhstan
* Corresponding author: lyazzatt@mail.ru

This paper belongs to the CTFM'22 Special Issue: https://www.kaznu.kz/en/25415/page.
Guest Editors: Prof. N. Uvarov and Prof. E. Aubakirov.

Abstract

Growing demand for hydrogen promotes the research devoted to the development of new catalysts for hydrocarbons processing in absence of H_2 or at its low concentration. In the present work, it was shown that during the conversion of straight-run gasoline on a zeolite-containing polyfunctional catalyst in a hydrogen-free environment cracking, dehydrogenation, isomerization and alkylation take place due to the redistribution of H_2 between initial and formed products directly on the catalyst surface. Fine particles (≤50 Å) localize in zeolite cavities and pores of aluminum oxide, while larger ones are on their outer surface.

Key findings

● High-octane gasoline containing 62.4% isoalkanes and 2.3% aromatic hydrocarbons is obtained on zeolite-containing catalyst at 350 °C with H_2:feedstock ratio = 200:1.

● Decrease in H_2:feedstock ratio to 50 leads to increase of hydrocracking direction, formation of aromatic hydrocarbons and olefins as well as C_{10}–C_{13} isoalkanes obtained as a result of a disproportionation reaction.

● Decrease in H_2:feedstock ratio leads to essential change in the composition of straight-run gasoline. The presence of aromatic hydrocarbons and olefins, which are octane-forming components, increases the motor properties of gasoline. C_{10}–C_{13} isoalkanes are the components of diesel fuel.

1. Introduction

Many processes at petrochemical and chemical plants are based on the use of hydrogen or hydrogen-containing gas (HCG) [1–3]. Due to the rapid growth of hydrogen energy application, the shortage and cost of hydrogen are increasing [4–8]; therefore, reducing the consumption of HCG by developing new catalysts and technologies is urgently needed [9–11].

In the literature [12–16] there are data on transformation of model n-alkanes over Pt/zeolite catalysts. During n-octane conversion on Pt/HY catalysts (t = 300 °C, P = 0.18 MPa, H_2/octane ratio is 16 mol.%), selectivity of isomers formation rises from 16.0% (0.02% Pt) up to

80.6% (10% Pt) with increasing platinum concentration. Under these conditions cracking direction decreases from 82.2 to 20.6% [17].

It was shown, that conversion of n-hexane over 0.3% Pt-containing zeolites of L and eryonite (E) type is influenced by the degree of ion exchange of K^+. Under the same conditions (t = 400 °C), the conversion of n-hexane increases from 26.1 to 47.0% with an increase in the degree of ion exchange from 17.0% to 82.0% in L zeolite. According to NH_3 adsorption, three types of acid centers with binding energy (q) equal to 100, 110 and 120 kJ/mol were determined in the catalyst. The highest activity in the n-hexane isomerization reaction is typical for the centers with q = 120 kJ/mol, while the acid centers with lower

binding energy also participate in hydro isomerization but with low efficiency [18]. Molecular sieve effect was shown when comparing the properties of catalysts containing L and E zeolites. On L-zeolite with wide pores (0.71 nm) isomer yield is greater than on E-zeolite with narrowpores (0.36x0.52 nm). In the latter case, the pores are not accessible to branched isomers.

In the present work, conversion of C_6–C_9 n-alkanes on Pt-Fe/Al_2O_3+HZSM catalyst modified with additives of cerium, molybdenum and phosphorus in the presence of H_2 was studied. Processing of straight-run gasoline was carried out with varying content of hydrogen and in its absence.

2. Experimental

The catalyst was prepared by impregnation of the Al_2O_3+HZSM mixture with water solutions of $Fe(NO_3)_3\cdot 9H_2O$, $(NH_4)_6Mo_7O_{24}\cdot 4H_2O$, $Ce(NO_3)_3\cdot 6H_2O$, H_2PtCl_6 and other salts. The wet catalyst sample was formed into granules, dried at 100–250 °C for 5 hours with a heating rate of 20–30 °C/min and calcined at 500 °C for 5 hours.

The tatalyst was studied in the reaction of transformation of C_6–C_9 n-alkanes and straight-run gasoline on the laboratory flow-through unit at the temperatures varying from 280 °C up to 400 °C, the hydrogen pressure of 2MPa, the H_2/feed ratio of 200/1, 50/1 and 0/1, and the volume feed rate of 5 h^{-1}. Hydrocarbon composition of the reaction products was analyzed on a "Chrom-4" chromatograph with a stainless steel column filled with γ- aluminum oxide by "Supelco". Argon was used as a carrier gas.

3. Results and discussion

The conversion and direction of C_6–C_9 n-alkanes transformation on the Pt(0.1%)-Fe(5%)/Al_2O_3+HZSM catalyst modified with various additives is affected by the process temperature under otherwise equal conditions (P_{H2} = 2MPa, V = 5 h^{-1}, H_2/feedstock ratio = 200/1). Table 1 shows the results obtained at n-nonane processing. As the temperature rises from 300 to 400 °C, the conversion of n-nonane increases from 51.2 to 93.6%.

As shown in Table 1, the olefins formed during dehydrogenation of intermediate activated surface complexes are rapidly isomerized through the carbonium ion formation and hydrogenated to isoalkanes. Due to this, only tracess of olefins are present in the products mixture. Other directions of olefins transformation probably include formation of aromatic hydrocarbons (0.1–2.7%) at temperatures of 350–400 °C. The maximum yield of C_4–C_8 isoalkanes (35.7%) is determined at 350 °C. The assumed mechanism of alkane conversion is possible on the active catalyst sites containing both metal and acid centers.

Figure 1 presents the data on C_6–C_8 n-alkanes conversion on the Pt-Fe/Al_2O_3+HZSM catalyst promoted by different additives and the yield of isomers at different temperatures.

With the increase in temperature, conversion of n-alkanes grows, and at 400 °C it reaches 96.7–97.9%. The temperature dependence of maximum yield of isomers is observed at close conversion degrees of C_6–C_8 n-alkanes. The curves pass through the extrema at 350–380 °C. The maximum yield (%) decreases in the following series: hexane (32.0%) > heptane (30.6%) > octane (30.3%). In the high temperature area (>350 °C) the formation of aromatic hydrocarbons (0.1–2.8%) and olefins (tracess) is observed.

Physical and chemical properties of the polyfunctional, promoted with additives, Pt (0.1%)-Fe(5%)/Al_2O_3+HZSM catalyst were studied by BET, XRD and electron microscopy (EM) methods. The specific surface area and total pore volume of the catalyst are 179.2 m^2/g and 0.40 cm^3/g, respectively. The XRD results show that the catalyst is dispersed. HZSM structural elements (reflexes 12.5; 10.9; 9.8; 3.83; 3.70; 3.64; 2.96 Å), Ce (reflex 2.76 Å) (ASTM 38-763), Pt (superimposed with γ-Al_2O_3, reflex 2.27 Å) (ASTM 4-802), ε-Fe_2O_3 (1.46 Å) (ASTM 16-895), γ-Al_2O_3 (reflexes 2.40; 1.98; 1.40) are present.

Table 1 Influence of temperature on n-nonane conversion on zeolite-containing Pt-Fe/Al_2O_3 catalyst (P = 2 MPa, V = 5 h^{-1}, H_2/feedstock ratio = 200).

Products composition, %	Temperature, °C				
	300	320	350	380	400
C_1–C_3 hydrocarbons	1.8	10.9	20.7	34.3	36.5
C_4–C_9 isoalkanes	20.2	30.9	35.7	33.2	31.5
C_4–C_8 n-alkanes	29.2	29.4	26.1	23.8	22.9
olefins	traces	traces	traces	traces	traces
aromatic hydrocarbons	–	traces	0.1	0.2	2.7
Feedstock	48.8	28.8	17.4	8.5	6.4
n-nonane conversion, %	51.2	71.2	82.6	91.5	93.6
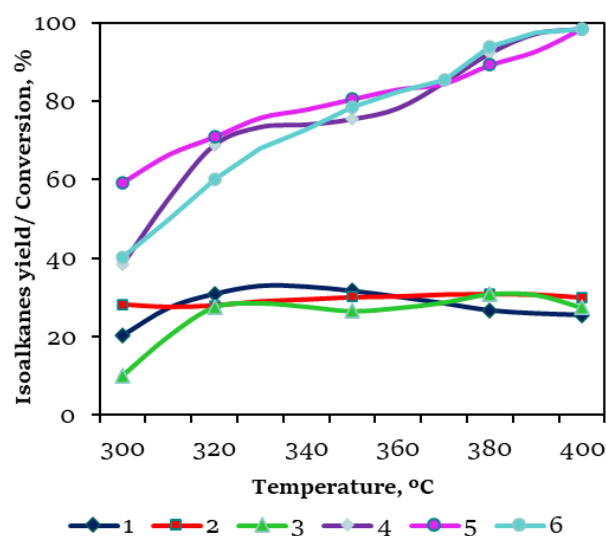
Figure 1 Influence of temperature on C_6–C_8 n-alkanes conversion and yield of isomers (P = 2 MPa, V = 5 h^{-1}, H_2:feed = 200:1). 1, 4 – Isoalkanes yield and conversion of n-hexane. 2, 5 – Isoalkanes yield and conversion of n-heptane. 3, 6 – Isoalkanes yield and conversion of n-octane.

The EM study (120000 magnification) showed the presence of an aggregate in the Pt-Fe/Al$_2$O$_3$ catalyst modified with cerium, molybdenum and phosphorus, which consists of dense particles of ~200 Å size. The micro diffraction pattern is represented by two rings and can be attributed to Fe$_2$O$_3$ Hematite (JCPDS, 35-664). At low magnification, large elastic lamellar crystals with basal reflections on their bends were detected. The micro diffraction pattern can be attributed to FeOOH (JCPDS, 26-792). Small loose clusters of dispersed particles with sizes of 20 Å were found in the sample; according to the micro diffraction pattern, they represent CeO$_2$ (JCPDS, 34-394). Small loose clusters of ~100 Å particles give a diffraction pattern which can be attributed to a mixture of Pt$_3$O$_4$, Mo$_9$O$_{26}$ (JCPDS, 21-1284) and CeAlO$_3$ (JCPDS, 28-260). Characteristic extensive clusters of 30–40 Å particles of Ce$_6$O$_{11}$ were detected. An aggregate of loose small particles 30–50 Å in size was found, which is a mixture of Ce(MoO$_4$)$_2$, Ce$_2$Mo$_3$O$_{12}$ and PtO$_2$ (JCPDS, 57-330). The sample also contains individual large dense crystals with cut features represented by the reflections with hexagonal arrangement, and they are related to FeMoO$_4$, CeP, β-MoO$_3$ (JCPDS, 37-1445), and PtO$_2$ (JCPDS, 23-1306).

Nanosized (20–100 Å) homo- and heteroatomic clusters were found in the zeolite-containing Pt(0.1%)-Fe(5%)/Al$_2$O$_3$ catalyst modified with phosphorus, molybdenum, and cerium additives. In the calcined catalyst (t = 500 °C), platinum (d = 30–100 Å) and iron (d = 200 Å) are in the form of oxides. Iron and cerium (d = 20–50 Å) interact with molybdenum, forming precursors (FeMoO$_4$, CeMoO$_4$, Ce$_2$Mo$_3$O$_{12}$), which transform into heteroatomic Fe–Mo and Ce–Mo nanoclusters in reducing medium.

Analysis of the obtained data on dimensionality and structure of metal particles of the catalyst active phase allows us to conclude that it is possible to synthesize nanocatalysts with given composition and properties by directed selection of precursors.

Presence of phosphorus in the catalyst prevents the formation of heteroatomic Pt–Fe, Pt–Mo clusters, whereas the introduction of molybdenum into the catalyst composition in the absence of phosphorus increases the dispersion of metal particles and promotes the formation of heteroatomic highly dispersed clusters at calcination. However, it cannot be excluded that such heteroatomic clusters may be formed during the hydrogen treatment of the catalyst (350–400 °C). Metal nanoparticles are localized in the cavity and mouths of zeolite and pores of aluminum oxide. In addition, larger 100–200 Å crystals were detected by electron microscopy method on the smooth surface of zeolite. It is known from the literature [19, 20] that reduction of iron (III) into iron (II) and iron (0) is observed under hydrogen treatment of air calcined Pt–Fe/Al$_2$O$_3$ – systems [19]. The formation of Pt–Fe clusters, which facilitates and accelerates the reduction of iron, was detected by NGRS method [20].

Zeolite-containing Pt(0.1%)-Fe(5%)/Al$_2$O$_3$-catalyst a modified with additives (Mo, Ce, P) were studied in the process of straight-run gasoline hydro refining at varying temperatures (280–400 °C), and H$_2$:feed ratio (pressure – 2 MPa, V = 5 h^{-1}).

At temperature rise from 280 up to 400 °C (P_{H2} = 2 MPa, V = 5 h^{-1}, H$_2$:feed=200:1), it was shown, that hydrocracking, hydro isomerization and dehydrocyclizationare occur on the catalyst at hydro refining of straight-run gasoline. The formation of light C$_1$–C$_3$–hydrocarbons occurs at t≥350 °C, and at 400 °C their yield is 17.6% (Table 2). The optimum yield of C$_4$–C$_9$ isoalkanes, 62.4%, was determined at 350 °C. At lower and at higher temperatures the yield of C$_4$–C$_9$ isoalkanes decreases to 50.5 and 51.3%. C$_{10}$–C$_{13}$ isoalkanes – 15.6%, C$_4$–C$_9$ n-alkanes – 15.3%, C$_{10}$–C$_{13}$ n-alkanes – 0.5% and aromatic hydrocarbons – 2.3% are also present in the product mixture. Olefins appear (0.3–0.4%) at temperatures ≥380 °C.

At straight-run gasoline hydro refining, attention was paid to the influence of H$_2$:crude ratio on the direction of the process. The data on straight-run gasoline conversion on the Pt-Fe/Al$_2$O$_3$ zeolite-containing catalyst at H$_2$:feed=50:1 are presented in Table 3. In this case, the process was carried out in the temperature range of 350–400 °C. The maximum hydro refining of straight-run gasoline occurs in these conditions. It follows from Table 3, that with H$_2$:feed ratio decreasing to 50/1 the isomerizing activity of the catalyst decreases from 62.4 to 54.3%.

Table 2 Conversion of straight-run gasoline on zeolite-containing Pt-Fe/Al$_2$O$_3$ catalyst (P = 2 MPa, V = 5 h^{-1}, H$_2$:feed=200:1).

Products composition, %	Process temperature, °C				
	280	300	320	350	380
C$_1$–C$_3$– hydrocarbons	–	–	traces	3.9	10.9
C$_4$–C$_9$ isoalkanes	50.5	54.7	56.7	62.4	54.2
C$_{10}$–C$_{13}$ isoalkanes	20.4	19.5	19.7	15.6	13.8
C$_4$–C$_9$ n-alkanes	26.9	23.3	21.1	15.3	18.7
C$_{10}$–C$_{13}$ n-alkanes	0.3	0.6	0.7	0.5	traces
aromatic hydrocarbons	1.9	1.9	2.0	2.3	2.1
olefins	–	–	traces	traces	0.3
Liquid phase yield	100	100	100	96.1	89.1

Table 3 Conversion of straight-run gasoline on zeolite-containing Pt-Fe/Al$_2$O$_3$ catalyst (P = 2 MPa, V = 5 h^{-1}, H$_2$:feed=200:1).

Products composition, %	Process temperature, °C		
	350	380	400
C$_1$–C$_3$– hydrocarbons	6.3	12.4	21.8
C$_4$–C$_9$ isoalkanes	54.3	49.9	42.5
C$_{10}$–C$_{13}$ isoalkanes	23.5	20.5	16.9
C$_4$–C$_9$ n-alkanes	8.1	9.9	11.6
aromatic hydrocarbons	7.5	6.9	6.7
olefins	0.3	0.4	0.5
Liquid phase yield	93.7	87.6	78.2

Hydrocracking with formation of C_1–C_3 hydrocarbons increases from 3.9 to 6.3% at 350 ºC. However, at a reduced H_2:feed ratio the yield of C_{10}–C_{13} isoalkanes rises from 15.6 to 23.5% (350 ºC). In all studied temperature range the yield of C_{10}–C_{13} isoalkanes is higher than at H_2:feed ratio = 200:1. The detected effect of a significant increase in the yield of aromatic hydrocarbons from 2.3 to 7.5% (Tables 2 and 3) is of particular interest. 0.3–0.5% of olefins were found in the products.

In order to elucidate more fully the role of HBG, the study of the catalyst activity in processing of straight-run gasoline in the absence of hydrogen was carried out. It was shown that the yield of C_4–C_9 isoalkanes at 350 ºC is 62.6%, and with the rise of temperature up to 400 ºC the content of isoalkanes in the product mixture falls to 39.0%. At the same time, there is a disproportionation reaction, which leads to C_{10}–C_{14} isoalkanes and C_{10}–C_{13} n-alkanes appearance. Their yields are maximal at 350 ºC (14.3% and 4.0% respectively). The most important is the formation of high-octane aromatic hydrocarbons – 5.4% (350 ºC) and olefins (6.7%).

4. Conclusions

Thus, in the absence of hydrogen the yield of C_4–C_9 isoalkanes is 62.6%, and heavier isoalkanes, aromatic hydrocarbons and olefins appear. Hydrocracking to C_1–C_3–hydrocarbons increases at high temperatures (380–400 ºC). At 350 ºC the yield of the liquid phase, i.e. gasoline with a sufficiently high octane number is close to 100%.

The analysis of the particle size of metals included in the catalyst shows that their dispersion varies within a wide range, from 20 to 200 Å. Fine particles (≤50 Å) can localize in zeolite cavities and pores of aluminum oxide, and large ones-on their outer surface. When the catalyst contacts with n-alkanes, the whole surface participates in the process, but formation of branched isomers of C_{6+} alkanes is possible only on the outer surface, whereas C_1–C_4 hydrocarbons of different structure probably appear in zeolite cavities during cracking transformation of n-alkanes capable of diffusing deep into the matrix structure. Diffusion of molecules and their transformation increase with temperature, which is confirmed by the increase in cracking of n-alkanes.

Supplementary materials

No supplementary materials are available.

Funding

Acknowledgments

Conflict of interest

The authors declare no conflict of interest.

Author contributions

Conceptualization: A.K.Z., L.K.T.
Data curation: A.K.Z.
Formal Analysis: L.K.T., Y.A.A.
Investigation: A.K.Z., L.K.T.
Methodology: R.O.O., Y.A.A.
Resources: R.O.O.
Supervision: Y.A.A.
Validation: A.K.Z., L.K.T.
Visualization: E.B.Z.
Writing – original draft: A.K.Z., E.B.Z.
Writing – review & editing: L.K.T.

Additional information

Author IDs:
Lyazzat K. Tastanova, Scopus ID 57202578243;
Raigul O. Orynbassar, Scopus ID 57223975563;
Yermek A. Aubakirov, Scopus ID 55447002200.

Websites:
Kazakh University of Technology and Business, https://kaztbu.edu.kz/;
K. Zhubanov Aktobe Regional University, http://zhubanov.edu.kz/en/;
Al-Farabi Kazakh National University, https://www.kaznu.kz/en.

References

1. Wu L, Liang XQ, Kang LX, Liu YZ. Integration strategies of hydrogen network in a refinery based on operational optimization of hydrotreating units. Chin J Chem Eng. 2017;25(8):1061–1068. doi:10.1016/j.cjche.2017.01.003
2. Bondarenko VL, Ilyinskaya DN, Kazakova AA, Kozlovtsev PS, Lavrov NA, Razenko EA. Hydrogen, its Unique Properties and Applications in Industry. Chem Pet Eng. 2022;57(11–12):1015–1019. doi:10.1007/s10556-022-01039-7
3. Pleshakova NA, Zanozina II, Shabalina OE, Rokhman'ko EN, Mishustina TV. Hydrofining of heavy vacuum gas oil on modified alumina-nickel-molybdenum catalysts. Pet Chem. 2012;52(4):233–239. doi:10.1134/S096554411204007X
4. Zhao GL, Nielsen ER, Troncoso E, Hyde K, Romeo JS, Diderich M. Life cycle cost analysis: A case study of hydrogen energy application on the Orkney Islands. Int J Hydrog Energy. 2019;44(19):9517–9528. doi:10.1016/j.ijhydene.2018.08.015
5. Tarasenko AB, Kiseleva SV, Popel OS. Hydrogen energy pilot introduction-Technology competition. Int J Hydrog Energy. 2022;47(23):11991–11997. doi:10.1016/j.ijhydene.2022.01.242
6. Hsu CW. Constructing an evaluation model for hydrogen application pathways. Int J Hydrog Energy. 2013;38(35):15836–15842. doi:10.1016/j.ijhydene.2013.05.100
7. Felseghi RA, Carcadea E, Raboaca MS, Trufin CN, Filote C. Hydrogen fuel cell technology for the sustainable future of stationary applications. Energies. 2019;12(23):4593. doi:10.3390/en12234593

8. Hashimoto K. Global carbon dioxide recycling: for global sustainable development by renewable energy. Springer Briefs in Energy. Springer: Singapore; 2019.89–90. doi:10.1007/978-981-13-8584-1_13

9. De Miranda PEV. Science and engineering of hydrogen-based energy technologies: hydrogen production and practical applications in energy generation. Elsevier: London; 2019.1–420.

10. Wang H, Lin, HF, Feng P, Han X, Zheng Y. Integration of catalytic cracking and hydrotreating technology for triglyceride deoxygenation. Catalysis Today. 2017;291:172–179. doi:10.1016/j.cattod.2016.12.009

11. Yin ZL. Operation and optimization of residue hydrotreating unit using new catalyst system. China Petroleum Process Petrochem Technol. 2012;14(3):50–58.

12. Sun JH, Li Y, Mu C, Wei J, Zhao YJ, Ma XB, Wang SP. Supported heteropolyacids catalysts for the selective hydrocracking and isomerization of n-C16 to produce jet fuel. Appl Catalysis A Gen. 2020;598:117556. doi:10.1016/j.apcata.2020.117556

13. del Campo P, Martinez C, Corma A. Activation and conversion of alkanes in the confined space of zeolite-type materials. Chem Soc Rev. 2021;50(15):8511–8595. doi:10.1039/d0cs01459a

14. Guisnet M, Pinard L. Characterization of acid-base catalysts through model reactions. Catal Rev Sci Eng. 2018;60(3):337–436. doi:10.1080/01614940.2018.1446683

15. Bi YF, Xia GF, Huang WG, Nie H. Hydroisomerization of long chain n-paraffins: the role of the acidity of the zeolite. RSC Adv. 2015;5(120):99201–99206. doi:10.1039/c5ra13784e

16. Jokar F, Alavi SM, Rezaei M. Investigating the hydroisomerization of n-pentane using Pt supported on ZSM-5, desilicated ZSM-5, and modified ZSM-5/MCM-41. Fuel. 2022;324(A):124511. doi:10.1016/j.fuel.2022.124511

17. Kuznetsov PN. Study of n-octane hydrocracking and hydroisomerization over Pt/HY zeolites using the reactors of different configurations. J Catal. 2003;218(1):12–23. doi:10.1016/S0021-9517(03)00139-8

18. Lapidus AL, Mentyukov DA, Dergachev AA. Isomeration of n-hexane on Pt-containing zeolites L and eryonite. Oil Refinery and Petrochemistry. 2005;7:9–12. [in Russian].

19. Zhumabekova AK, Tastanova LK, Orynbassar RO, Zakumbaeva GD. Effect of modifiers on Fe-Pt/Al$_2$O$_3$ catalysts for alkanes hydrotreatment. Bull Univ Karaganda Chem. 2020;100:104–118. doi:10.31489/2020Ch4/104-118

20. Li XN, Zhu KY, Pang JF, Tian M, Liu JY, Rykov AI, Zheng MY, Wang XD, Zhu XF, Huang YQ, Liu B, Wang JH, Yang WS, Zhang T. Unique role of Mossbauer spectroscopy in assessing structural features of heterogeneous catalysts. Appl Catal B-Environ. 2018;224:518–532. doi:10.1016/j.apcatb.2017.11.004